



Provided by the author(s) and University of Galway in accordance with publisher policies. Please cite the published version when available.

Title	Effects of viscosity and refractive index on the emission and diffusion properties of Alexa Fluor 405 using fluorescence correlation and lifetime spectroscopies
Author(s)	van Zanten, Camila; Melnikau, Dzmitry; Ryder, Alan G.
Publication Date	2021-03-19
Publication Information	van Zanten, Camila, Melnikau, Dzmitry, & Ryder, Alan G. (2021). Effects of Viscosity and Refractive Index on the Emission and Diffusion Properties of Alexa Fluor 405 Using Fluorescence Correlation and Lifetime Spectroscopies. <i>Journal of Fluorescence</i> , 31(3), 835-845. doi: 10.1007/s10895-021-02719-y
Publisher	Springer
Link to publisher's version	https://doi.org/10.1007/s10895-021-02719-y
Item record	http://hdl.handle.net/10379/18127
DOI	http://dx.doi.org/10.1007/s10895-021-02719-y

Downloaded 2024-05-19T17:58:24Z

Some rights reserved. For more information, please see the item record link above.



Citation: Effects of viscosity and refractive index on the emission and diffusion properties of Alexa Fluor 405 using fluorescence correlation and lifetime spectroscopies., C. van Zanten, D. Melnikau, and A.G. Ryder. *Journal of Fluorescence*, 31(3), 835-845, (2021).
DOI: [10.1007/s10895-021-02719-y](https://doi.org/10.1007/s10895-021-02719-y)

1
2 **Effects of viscosity and refractive index on the emission and diffusion properties of Alexa**
3 **Fluor 405 using fluorescence correlation and lifetime spectroscopies.**

4
5 Camila van Zanten,¹ Dzmitry Melnikau,¹ and Alan G. Ryder^{1*}.

6
7 ¹School of Chemistry, National University of Ireland, Galway, University Road,
8 Galway, H91 CF50, Ireland.

9
10
11 * Corresponding author.

12 Prof. Alan G. Ryder, Nanoscale Biophotonics Laboratory, University of Galway, Galway,
13 H91TK33, Ireland.

14
15
16
17
18
19
20
21
22
23
24
25
26
27
28
29
30
31
32
33
34
35
36
37
38
39
Tel: 353-91-492943

Fax: 353-91-552756

Email: alan.ryder@universityofgalway.ie

ORCID:

C. Van Zanten: 0000-0002-5827-8561

D. Melnikau: 0000-0002-6588-8122

A. G. Ryder: 0000-0002-3133-4340

Abstract:

Fluorescence Correlation Spectroscopy (FCS) studies of the interaction of polymers or proteins in solution are strongly affected by the viscosity and refractive index of the medium, and the effects are likely to be more significant with the use of short wavelength excitation (e.g., 405 nm diode lasers). Failing to account for these issues can lead to incorrect measurement of average size, conformational changes, and dynamic behaviour of polymers and proteins. Steady-state, time-resolved, and FCS measurements of Alexa 405 in glycerol:water mixtures were performed to determine its suitability for FCS measurements with 405 nm excitation. The effects of the refractive index and viscosity on the diffusion coefficient and photophysical parameters (lifetime and relative quantum yield) of the fluorophore were determined. Alexa 405 lifetime decreased from 3.55 ns in water to 3.25 ns in a 50:50 glycerol:water mixture, while its diffusion coefficient dropped from 333 ± 16 to $44 \pm 1 \mu\text{m}^2\text{s}^{-1}$. Lifetime data collected from micromolar solutions of Alexa 405 did however also suggest that as solvent polarity decreased, aggregates (excimers) were formed as evidenced by the appearance of a rising edge in the decay plots. The interdependence between lifetime, refractive index, and diffusion coefficient could be accurately fitted by a simple polynomial function indicating that the probe is well behaved and predictable in the glycerol:water model system. Overall, Alexa 405 is a most promising and reliable probe for FCS measurement using violet laser diode excitation sources.

Citation: Effects of viscosity and refractive index on the emission and diffusion properties of Alexa Fluor 405 using fluorescence correlation and lifetime spectroscopies., C. van Zanten, D. Melnikau, and A.G. Ryder. *Journal of Fluorescence*, 31(3), 835-845, (2021).
DOI: [10.1007/s10895-021-02719-y](https://doi.org/10.1007/s10895-021-02719-y)

1
2
3
4
5
6
7
8
9
10

Key Words: Fluorescence Correlation Spectroscopy; fluorescence lifetime; Alexa Fluor 405; diffusion coefficient; viscosity; refractive index;

Open Access Version: Note that this is the final accepted version which has not been proof corrected or typeset by the publisher. The item of record is the published version.

1

2 **Introduction**

3 Fluorescence Correlation Spectroscopy (FCS) is widely used in biology and life
4 sciences and encompasses processes such as the diffusion and transport of proteins in the
5 cellular environment [1], determination of equilibrium binding constants between proteins and
6 substrates [2], the detection of protein aggregates in live cells [3], and assessment of cellular
7 uptake, distribution and degradation of peptides [4]. More recently, FCS has been used to study
8 protein dynamics [1,5] and polymeric nanoparticles [6,7] in solution, and at how proteins
9 behave when interacting with polymer nanoparticles. FCS has been used to determine the
10 effect of NP size on the magnitude of the protein-adsorbed fraction [8], and protein diffusion
11 within crowded polymer solutions [9].

12 However, FCS investigations of the interactions of proteins in live cells or in crowded
13 polymeric environments can result in measurement issues related to changes of local viscosity
14 and refractive index. Viscosity and refractive index can vary significantly in micro-
15 heterogeneous systems such as cellular environments [10] and polymeric solutions [11]. In the
16 latter, the very large size of some polymer macromolecules can significantly alter the local
17 viscosity of the medium, even in dilute concentrations [11]. The viscosity felt by the probe in
18 polymer solutions depends ultimately on the ratio between the effective probe size and the
19 polymer correlation length (ξ) [12]. High concentration polymer and protein solutions are of
20 significant interest for drug formulation of both large and small molecule Active
21 Pharmaceutical Ingredients (APIs)[13-16]. In addition to the length scale-dependent viscosity,
22 one also needs to investigate the impact of refractive index (RI) changes in these concentrated
23 polymer solutions on the emission and FCS data and therefore on any recovered parameters.
24 RI variations in the sample solution, can lead to spherical aberrations which distort the
25 measured fluorescence signal which leads to artefacts in the measured autocorrelation function
26 (ACF). This can lead to the calculation of erroneous values for fluorophore concentration and
27 diffusion coefficient [17-19]. These problems can largely be eliminated, if one is aware of RI
28 changes in the sample, by using the correction collar (CC) of the objective lens and by selecting,
29 and fixing an appropriate depth of focus [20].

30 Modern confocal microscopes often have multiple excitation sources available to
31 enable multiple labelling of proteins for a wide variety of applications such as colocalization
32 [21,22] and Förster Resonance Energy Transfer (FRET) studies [22,23]. 405 nm diode lasers
33 are now a common excitation source used to excite fluorophores like DAPI [24,25], Hoechst
34 [22,23], and Atto 390 [26]. The use of 400-405 nm excitation for FCS is rare, but it has been
35 used for studying blinking processes in fluorescent proteins and fluorophore stability [24,25].
36 For more common, diffusion measurement-based FCS applications, the use of UV excited
37 fluorophores is not so widespread for a number of reasons including: biological phototoxicity,
38 photobleaching, significantly increased scatter, and also because of the limited number of
39 bright and stable fluorophores in this spectral range. In additional, quantitative FCS
40 measurements require a confocal volume of well-known dimensions for precise data fitting
41 [27], which is usually done by calibrating the confocal volume V_{conf} with a fluorophore of

Citation: Effects of viscosity and refractive index on the emission and diffusion properties of Alexa Fluor 405 using fluorescence correlation and lifetime spectroscopies., C. van Zanten, D. Melnikau, and A.G. Ryder. *Journal of Fluorescence*, 31(3), 835-845, (2021).
DOI: [10.1007/s10895-021-02719-y](https://doi.org/10.1007/s10895-021-02719-y)

1 known diffusion coefficient. However, there is currently a lack of reliable fluorophores with
2 known data suitable for instrument calibration at or near 405 nm.

3 Despite all these drawbacks, there is potential utility in using these shorter wavelength
4 excitation sources for the analysis of high concentration polymer solutions, as the Rayleigh/Mie
5 scatter can provide a useful source of additional information for characterising these types of
6 sample. Alexa 405 is marketed as a bright and stable fluorophore over a wide pH 4 to 10 range
7 with absorption/emission maxima at 402/422 nm, respectively. Here we investigated in detail
8 its potential as a fluorophore for viscosity studies by both ensemble and single-molecule
9 fluorescence techniques. We use glycerol:water mixtures as a model for varying the viscosity
10 and study the impact of changing refractive index on emission parameters.
11

12 **Methodology**

13 **Materials and sample preparation:** Alexa Fluor 405 (NHS ester) and Coumarin 102 98%
14 were purchased from ThermoFisher and Sigma, respectively. High purity water (HPW) was
15 purchased from Honeywell, Glycerol 99.5+% spectroscopic grade was purchased from Acros
16 Organics, and ethanol was purchased from Fisher Scientific. Ludox AS-40 40%wt suspension
17 in water and Atto 425 carboxylic acid were purchased from Sigma-Aldrich. Fluorophores and
18 solvents were used as received without further purification. Stock solutions of Alexa 405 (2
19 μM) and Atto 425 (30 μM) were made up in HPW and diluted as required. Glycerol was used
20 as the co-solvent in the aqueous solutions of Alexa 405. For the confocal volume calibration,
21 10 nM solutions of Atto 425 in HPW were used. For all FCS measurements samples were held
22 in 8 well chambered cover slides (Nunc® Lab-Tek® II Chamber Slide™ Fisher Scientific).
23 For lifetime and FCS measurements, 1.2 μM and 10 nM solutions, respectively, of Alexa 405
24 were prepared in triplicate in HPW and in 1:9, 2:8, 3:7, 4:6, and 5:5 glycerol:water mixtures.
25 The glycerol:water solutions were designated 0:1 (pure HPW), 1:9 for 10 % glycerol
26 (percentage volume), 2:8 for 20% glycerol, and so on. Thus the 50:50 glycerol:water mixture
27 represents a 20% glycerol mole fraction.

28 Quantum yield measurements of Alexa 405 were made in water and glycerol:water mixtures
29 using Coumarin 102 in ethanol as a quantum yield standard following the procedure set out in
30 an IUPAC protocol [28]. This involved preparing a 2 μM solution of Coumarin 102 in ethanol,
31 1.2 μM solutions of Alexa 405 in water, and in the glycerol:water mixtures. These
32 concentrations were selected to ensure low absorbance (< 0.08) and avoid inner filter effects
33 (IFE). All solutions were measured in triplicate and spectral data was corrected for refractive
34 index, but not for refractive index dispersion over the spectral range.
35

36 **Instrumentation:** Fluorescence lifetime data were collected at room temperature with a
37 FluoTime 200 time resolved spectrometer (PicoQuant, Berlin) using a 405 nm pulsed diode
38 laser (LDH-P-C-400) excitation source. A 10 MHz repetition rate was used and a band pass
39 filter (405 ± 10 nm) was used for the excitation beam. Fluorescence was detected at 422 nm
40 at the magic angle with 16 nm bandpass slits. A diluted Ludox solution (a pure scatterer) was
41 used to collect the Instrument Response Function (IRF). Data was collected until the channel

Citation: Effects of viscosity and refractive index on the emission and diffusion properties of Alexa Fluor 405 using fluorescence correlation and lifetime spectroscopies., C. van Zanten, D. Melnikau, and A.G. Ryder. *Journal of Fluorescence*, 31(3), 835-845, (2021).
DOI: [10.1007/s10895-021-02719-y](https://doi.org/10.1007/s10895-021-02719-y)

1 of maximum intensity has a minimum of 10k counts and the decay curves were fitted by
2 reconvolution using the Fluofit software (PicoQuant).

3 Electronic absorption spectra (200-700 nm range) were collected using a Cary 60 UV-Vis
4 spectrophotometer (Agilent) equipped with a temperature-controlled sample cell.
5 Fluorescence spectra were measured using a Cary Eclipse (Agilent) fluorescence
6 spectrophotometer fitted with a temperature-controlled cell holder. UV and fluorescence
7 spectra were collected at 20 °C using 10×10 mm pathlength quartz cuvettes (Lightpath Optical,
8 UK).

9
10 **FCS experimental:** FCS measurements were made using an Alba fluorescence fluctuation
11 spectroscopy system (ISS, Champaign Illinois) coupled to an Olympus IX71 confocal
12 microscope equipped with a UPlanSApo 60× NA 1.2 water immersion objective (Olympus).
13 The excitation source was a 405 nm pulsed diode laser (PicoQuant LDH-P-C-400, 390-420
14 nm) operated at a 20 MHz repetition rate using a PDL 800-D picosecond diode laser driver.
15 Laser power at the sample was kept between 11 and 12 μW (measured just above the objective
16 lens). Excitation light was directed by fibre optics into the inverted epifluorescence microscope
17 and then via a 405 bandpass filter (Semrock) into the dichroic mirror (Di02-R405-25×36,
18 Semrock) before reaching the objective lens. The fluorescence emission was filtered through
19 a 405 nm long pass filter (Semrock) then split 50:50 by a beam splitter and sent through two
20 50 μm diameter pinholes into two avalanche photodiode detectors (APDs). The signals were
21 autocorrelated using an SPC-150 correlator card (Becker & Hickl, Berlin). A control sample
22 of HPW was measured under the same experimental conditions to determine the noise floor,
23 which has a contribution from the Raman water band (occurs at ≈ 470 nm). The background
24 signal was negligible. The FCS data was analysed using both the analysis software supplied
25 by ISS (VistaVision ver. 4.2.148) and PyCorrFit, a freely available software package [29]. All
26 measurements were made at room temperature, which was 20 ± 1 °C and controlled via the
27 laboratory air conditioning.

28
29 **Modelling:** Strickler and Berg [30] proposed a formula that relates how the radiative decay
30 rate of a fluorophore varies according to the RI of the surrounding medium, when the only
31 mechanism of deactivation is spontaneous emission from the excited state. Theoretical
32 radiative lifetimes τ_{calc} were calculated at a wavelength of 422 nm (corresponding to the
33 emission maximum of Alexa 405) using the Strickler-Berg equation (see SI for details of
34 calculations). The refractive index at 422 nm was calculated for each glycerol:water solution
35 using the equation devised by Toptygin *et al.* [31] (see SI for details), as we did not have
36 instrumentation available to make measurements at this wavelength. In order to test if this
37 equation (Equation S-5, SI) provided a reliable estimate for the refractive index at 422 nm and
38 20 °C, we calculated the RI for a wavelength of 589 nm (at T = 20 °C) and then compared these
39 values with the experimentally measured RI values obtained using a commercial refractometer
40 with a 589 nm source. The agreement between theoretical and experimental values was fairly
41 good with relative errors of 0.16, 0.29, 0.42, 0.53, and 0.64% for the mixture ratios 1:9, 2:8,
42 3:7, 4:6, and 5:5, respectively. Therefore, we have a good expectation that our calculated

1 refractive index values for 422 nm are sufficiently accurate. However, we also need to point
2 out that several other factors apart from refractive index also play a part in the emission process,
3 they are: solvent polarity, rate of solvent relaxation, solvent hydrogen bond donor and hydrogen
4 bond acceptor ability. In particular the hydrogen bonding interactions between water and
5 glycerol are not straightforward, particularly near the 50:50 vol% concentration (20% mole
6 fraction of glycerol) [32]. Investigating the solvent contributions to Alexa 405 emission was
7 not the purpose of this study, as it was considered to be outside the scope of
8

9 **3. Results and discussion**

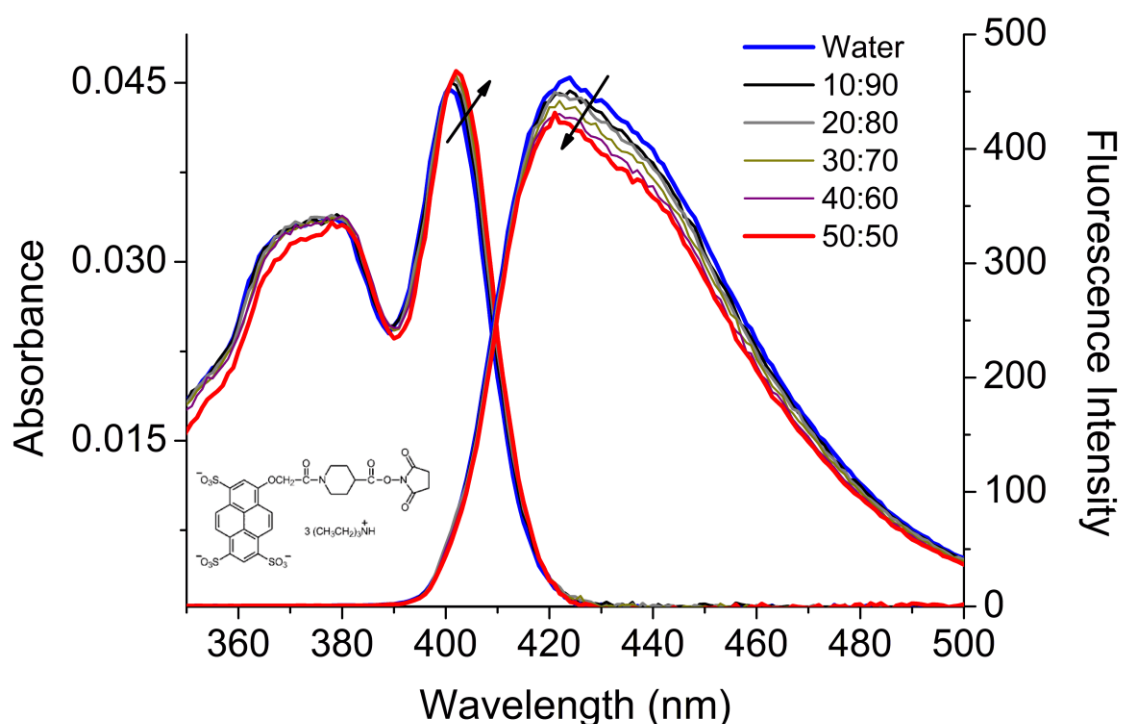
10 Our objective in this work was to select a fluorophore suitable for undertaking FCS
11 measurements in polymer solutions using 405 nm excitation. The goal is to use this excitation
12 wavelength for multi-parameter analysis with light scatter measurements for turbidity and
13 particle size changes of non-fluorescent components, fluorescence for FCS analysis of specific
14 components, and FRET analysis of specific interactions [33]. After evaluating the available
15 fluorophores, we selected Atto 390, Atto 425, and Alexa 405 for further study. The Atto
16 fluorophores suffered from significant photobleaching with laser excitation of 8 μ W. Lowering
17 the excitation power to \sim 6.5 μ W reduced photobleaching, however, we still consistently
18 recovered lower Atto concentrations from FCS measurements compared to equivalent
19 measurements made with Alexa405. This strongly suggested that the Atto fluorophores in
20 aqueous solutions were being adsorbed onto the polystyrene walls and borosilicate glass floor
21 of the sample chambers. Later when PNIPAm was added to Atto solutions it was observed
22 that the correct fluorophore concentration was measured when using PNIPAm concentrations
23 of $>$ 2.0 wt% (**Table S1, SI**). PNIPAm's affinity for glass and polystyrene is well documented
24 [34-36], which suggests that it preferentially coats the chamber surfaces and thus increases
25 fluorophore solution concentration. This surface adsorption loss process was not observed for
26 Alexa 405 and thus this fluorophore was selected as being the best candidate for studying future
27 polymer-fluorophore interactions and size measurements where fluorophore concentration is a
28 critical measurand.
29

30 **3.1 Steady-state and time-resolved fluorescence measurements.**

31 For practical purposes, in studies involving fluorophores in viscous, polymer systems, it is
32 important to understand in detail how solution properties affect the fluorescence lifetime,
33 spectrum, quantum yield (ϕ), and stability of the fluorophore. Here we analysed the steady-
34 state and time-resolved properties of Alexa Fluor 405 in glycerol:water mixtures of increasing
35 viscosity. The use of increasing volume fractions of glycerol, from 10 to 50% changes several
36 additional factors such as refractive index, rate of solvent relaxation, hydrogen bonding, and
37 solution polarity which will impact emission properties. Figure 1 shows the absorption and
38 emission spectra of Alexa 405 in all the various solutions. A slight hypsochromic shift (Figure
39 1) and decrease in emission intensity (around \approx 8%) were observed for the glycerol:water
40 mixtures. This effect was caused by a decrease in polarity, and changing solvent properties
41 (e.g. decrease in permittivity, changing hydrogen bond donor and acceptor ability), with

1 increasing glycerol concentration [37,38]. It should be noted that the absorbance
2 measurements were made with a 1 cm pathlength cell resulting in maximum absorbances of
3 ~0.04 which is too close to the photometric accuracy (± 0.01) and reproducibility (± 0.003 ,
4 standard deviation for 10 measurements) of this spectrometer. It was also noticed that the
5 spectra became progressively noisier as the glycerol content was increased. In retrospect, it
6 would be preferable to use a longer pathlength cell for absorbance measurements to reduce
7 measurement error.

8
9



10 **Figure 1.** Absorption and fluorescence spectra of Alexa 405 in water and in the glycerol:water
11 mixtures at 20 °C, all at 1.2 μM concentration (spectra are uncorrected). The inset plot shows the
12 chemical structure of Alexa 405 that has an extinction coefficient in water of $\epsilon = 3.5 \times 10^4 \text{ M}^{-1} \text{ cm}^{-1}$
13 at 402 nm according to the manufacturer.

14
15 Figure 2a shows the fits to the fluorescence lifetime decays acquired from the different
16 Alexa solutions. The fluorescence lifetime decay of Alexa 405 (micromolar or nanomolar
17 concentrations) in water fitted to a single exponential decay with $\tau = 3.56 \pm 0.02 \text{ ns}$, which
18 agreed with values published by Racknor et al. [39] of 3.57 ns. The data measured for nM
19 solutions of Alexa405 all fitted to a single exponential (Table 1 and **Table S2, SI**), however,
20 in solutions containing glycerol measured at a higher, micromolar, concentration all had to be
21 fitted with a bi-exponential decay (**Table S3 and Figure S-1, SI**). The second lifetime
22 component had a negative amplitude, the magnitude of which increased as the glycerol
23 concentration increased. This rise time is indicative of the formation of some form of aggregate
24 [40] (presumably an excimer) in these higher concentration solutions. The fact that the pyrene
25 core of Alexa 405 has three SO_3^- groups (inset in Figure 1) indicates that the fluorophore is

1 relatively hydrophilic. As the glycerol concentration increases one would expect that the water
2 in the water solvation shell becomes increasingly compacted and then gets displaced by
3 glycerol, resulting in a reduction in the Stokes shift and lifetime [41]. Furthermore, as the
4 solvent polarity reduces then the probability of fluorophore aggregation should also increase,
5 resulting in the formation of a faster lifetime excimer.

6 The differences in the recovered Alexa 405 monomer lifetime for the nM (Table 1 and
7 **Table S2, SI**) and μ M (**Table S3, SI**) concentrations were negligible. The lifetime of Alexa
8 405 drops from 3.56 ns in pure water to 3.29 ns in the 5:5 glycerol:water mixture (in nM
9 concentration, Table 1), which was expected due to the refractive index effect. This was
10 modelled using the Stricker-Berg relationship (Figure 2b) and showed a linear dependency for
11 both these lifetimes with $1/n^2$.

13 **Table 1.** Effect of changes in refractive index on the fluorescence decay (calculated and
14 experimental), and the relative quantum yield, of Alexa 405 at 20 °C. N = 6 for experimental
15 lifetime results.

Mixture	Glycerol vol. %	$n^a_{(\text{calc})}$	τ_{exp}^b (ns)	$\tau_{r\text{calc}}^c$ (ns)	Φ_{rel}^d
water	0	1.342	3.56±0.02	4.43±0.005	0.93±0.01
1:9	10	1.357	3.53±0.02	4.35±0.021	0.93±0.02
2:8	20	1.371	3.47±0.02	4.26±0.015	0.94±0.02
3:7	30	1.387	3.42±0.02	4.14±0.010	0.94±0.01
4:6	40	1.402	3.34±0.02	4.06±0.015	0.94±0.02
5:5	50	1.416	3.29±0.02	3.97±0.005	0.94±0.03

16 ^aRefractive indices calculated at the emission maximum of Alexa 405 (422 nm) for 20 °C according to
17 reference [31]; ^bExperimental lifetime (10 nM conc., mono-exponential decay), the error is the average
18 of the confidence interval reported by the fitting software; ^cTheoretical Radiative lifetime calculated
19 using the Strickler-Berg equation; Measured relative to Coumarin 102 in ethanol.

21 The experimental lifetime values, $\tau_{r\text{calc}}$, were $\approx 22\%$ lower than the predicted lifetimes
22 presumably due to non-radiative decay processes, which varied according to solvent composition
23 because the two slopes were not identical. The predicted and experimental decreases in lifetime
24 were also a bit different over the sample range with the theoretical values predicting a 10%
25 decrease whereas the experimental values were 8% (similar to the intensity decrease). This
26 might suggest that another factor was affecting the lifetime such as solvation effects or oxygen
27 quenching. Oxygen quenching is possible, as all solutions were not degassed, however, this did
28 not agree with the quantum yield data which showed no decrease. The lifetime changes
29 combined with the small reduction in the Stokes shift (bathochromic absorption and
30 hypsochromic emission) could indicate a small degree of excited state destabilization due to
31 changing solvation of the Alexa molecule.

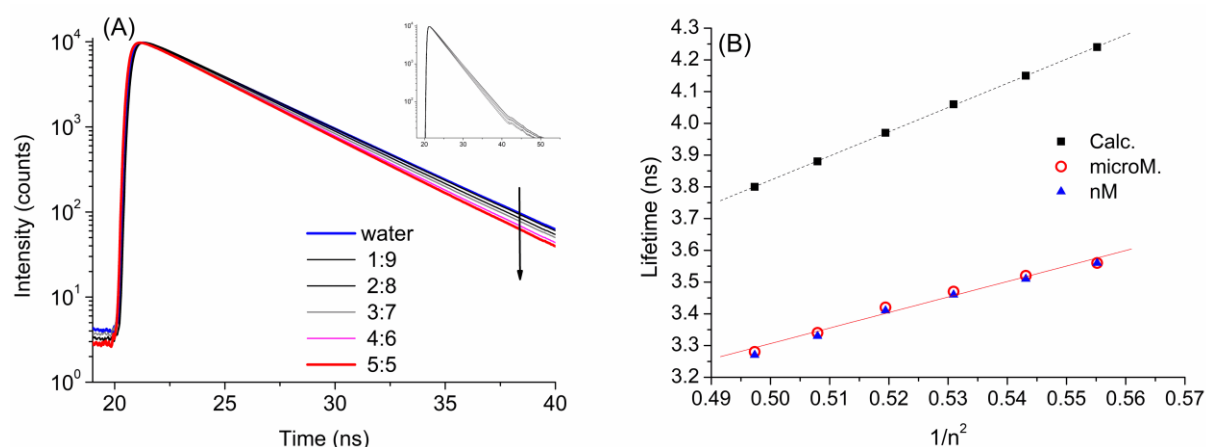


Figure 2. Left: Fluorescence lifetime decays of Alexa 405 (1.2 μM) in water and glycerol:water mixtures from 10 to 50% in volume (1:9 to 5:5). Inset shows the full decay curves. **Right:** Plot of calculated (black squares) and experimental (open circles μM, blue triangles nM) fluorescence lifetimes of Alexa 405 versus the inverse of the refractive index squared (values calculated at 421 nm) for the solutions of varying glycerol content (from 0 to 50 vol%). The calculated values (black squares) fit equation is $y=0.00602+7.62974x$, $r^2=0.998$, while the experimental values fit equation is $y=0.86334+4.88594x$, $r^2=0.982$ (μM)

Alexa 405's quantum yield (ϕ) in water and in aqueous glycerol solutions has not yet been reported to the best of our knowledge. Here we measured the relative quantum yield by comparison with coumarin 102 a standard of known ϕ (see SI for the formula) using an IUPAC recommended method [28]. Coumarin 102 in ethanol was selected due to its relatively high quantum yield of 0.76 [42], and emission wavelength range, 430-530 nm, which best overlapped that of Alexa 405 when compared to other fluorophores that absorb at around 400 nm (see Figure S2, SI for the superimposed absorption and emission spectra of Alexa 405 and Coumarin 102). The relative quantum yield of Alexa 405 showed a very small increase (Table 1) from pure water (0.93) to the 50% glycerol solution (0.94). This very small increase (~1.5%) is of the same magnitude of the measurement error here, and thus essentially constant. The apparent contradiction with the observed lifetime and spectral intensity could be explained by a change in the radiative decay rate. This could be caused by a decrease in solvent dielectric permittivity (polarity) [35, 43] with increasing glycerol content [41]. A decreasing lifetime with a concomitant slight increase in quantum yield has been observed for the emission from a single tryptophan residue in a protein when in varying glycerol-water solutions [31]. Overall, apart from the lifetime, the emission parameters for Alexa 405 are relatively stable over these glycerol water mixtures, which suggest that the fluorophore should be suitable for FCS over this viscosity range.

We do have to note here that glycerol contained a fluorescent impurity (detected using both FCS and fluorescence spectroscopy). However, because nearly all spectroscopy measurements used micromolar fluorophore concentrations the contribution of the known, low-concentration fluorescent impurity had little impact. This fluorescent impurity in glycerol which have been reported before, in our laboratory [43] and elsewhere [44-46] was confirmed by measuring an excitation-emission matrix (EEM) measurements of the blank glycerol:water

1 mixtures (**Figure S3, SI**). The EEM shows that at 405 nm excitation there was significant
2 emission generated in the 400–500 nm range by the impurity. The emission was ~40% as
3 intense as the Rayleigh scatter and this was further confirmed via single molecule
4 measurements (*vide infra*). For the lifetime measurements using nanomolar concentrations the
5 slit widths and monochromator settings ensured that the contribution of the impurity
6 fluorescence was minimal and had no impact on the recovered lifetimes. However, all FCS
7 measurements were made using nanomolar concentrations and the detection channels used long
8 pass filters to collect more emission wavelengths and thus the impurity contribution needs to
9 be accounted for.

11 **3.2 FCS of Alexa 405 in water:**

12 In quantitative fluorescence microscopy, accurate knowledge of the dimensions of the confocal
13 volume is of paramount importance, and this is particularly important for reliable extraction of
14 data in FCS and PCH-based measurements. The use of stable, bright fluorescent standards
15 with known diffusion coefficient, D_{coeff} , is the most convenient and common method for
16 measuring the confocal volume, V_{conf} , for one photon excitation sources in FCS measurements
17 [27]. The use of diode laser sources emitting at 400–405 nm in cytometry and imaging
18 applications is widespread [47,48] but there is a lack of relevant literature on fluorophore
19 standards with known diffusion coefficients for calibration of the confocal volume when violet
20 lasers are used. Atto 425 is one of the few fluorophores with a published D_{coeff} (438 ± 90
21 $\mu\text{m}^2\text{s}^{-1}$)[49] that can be excited at 400 nm. This was used to calibrate the confocal volume of
22 our instrumentation to enable the measurement of an accurate diffusion coefficient for Alexa
23 405 which has not been reported previously. It should also be noted that if stored in water (as
24 was the case here), hydrolysis of the ester portion of Alexa 405 occurs and the predominant
25 form of the molecule in solution, considering co-diffusion of the molecule and its counterions,
26 has a MW of 930 g/mol (See Figure S5, SI for a scheme of the hydrolysis reaction).

27 Measurements with Atto 425 in water (10 replicate measurements) and fitting the data
28 to the theoretical ACF (using literature values), we obtained the following values for the lateral
29 and axial radii: $w_0=0.38\pm 0.01$, and $z_0=2.1\pm 0.4$, which gave a structural parameter, z of 5.5. V_{eff}
30 was calculated to be 1.7 ± 0.2 fL with a corresponding V_{conf} of 0.60 ± 0.08 fL (see **SI** for details
31 of calculations). This data was then used for determining D_{coeff} for Alexa 405 in water for
32 which the experimental data was fitted using two different software programs (VistaVision,
33 which is the ISS fitting software and PyCorrFit developed by Muller *et al.* [50]). In all cases,
34 the data was fitted to a single species. D_{coeff} was calculated to be $333\pm 10 \mu\text{m}^2\text{s}^{-1}$ ($n=57$) and
35 $333\pm 16 \mu\text{m}^2\text{s}^{-1}$ ($n=57$) using PyCorrFit and VistaVision respectively (see **Figure S4, SI**).
36 These values for Alexa 405 were consistent with literature values for similar fluorophores.
37 Štefl *et al.* [49] determined the diffusion coefficient of Atto 425 as $438 \mu\text{m}^2\text{s}^{-1}$ (MW=401.45
38 g/mol), while Muller *et al.* [51] obtained $407 \mu\text{m}^2\text{s}^{-1}$ for Atto 655 maleimide (MW=812 g/mol).
39 Furthermore, comparison of the molecular masses of Atto 425 and the hydrolysed form of
40 Alexa 405, suggests that there should be a 1.26-fold decrease in the D_{coeff} . When we applied
41 this decrease to the reference D_{coeff} of Atto 425 ($438 \mu\text{m}^2\text{s}^{-1}$) we obtained $324 \mu\text{m}^2\text{s}^{-1}$, which
42 agrees with our experimentally determined values within experimental error.

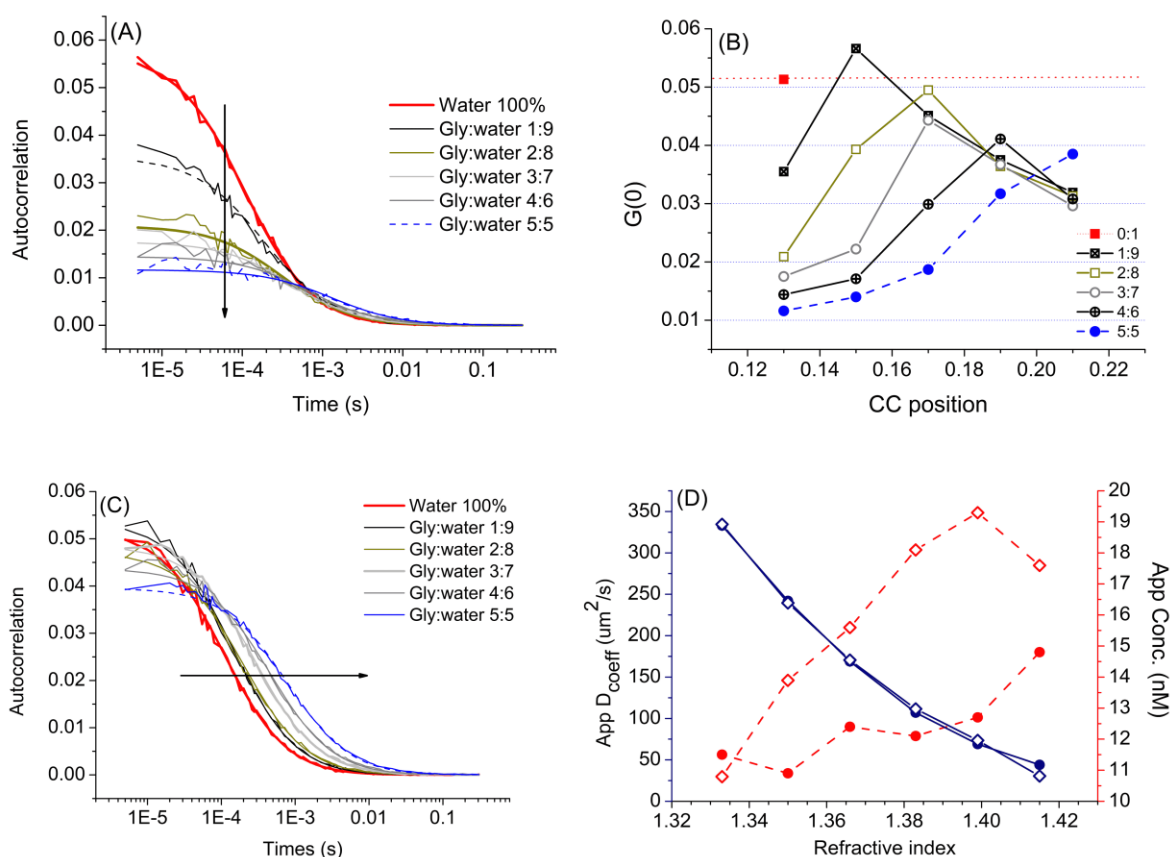
1
2
3
4
5
6
7
8
9
10
11
12
13
14
15
16
17
18
19
20
21
22
23
24
25
26
27
28
29
30
31

3.3 FCS of Alexa 405 in viscous solutions:

The water glycerol model is a common system for validating viscosity measurements. Here we wanted to assess the suitability of Alexa 405 for viscosity measurements, and in particular assess the impact of the associated refractive index changes [19,52]. This effect has been previously studied at longer excitation wavelengths (e.g. 488 nm [20] and above), but there is little information available for 400-405 nm excitation. Typically, the RI will increase by between 0.2% (water) and 0.4% (glycerol) on going from 488 to 405 nm excitation which will change the depth of focus. A second issue is that the degree of scatter will increase much more dramatically than this, making any misalignment due to mismatch much more serious in terms of fluorescence signal quality. Therefore for 405 nm based FCS, the correct use of the correction collar (CC) is more critical to avoid generating additional, unwanted scatter signal [51]. The issue is further complicated when one deals with samples of varying RI, for example, here the RI change (measured at 589 nm),¹ was very significant, $\approx +5\%$, on moving from pure water (1.333) to 50% glycerol (1.415). All of these factors will contribute to changing the quality of the collected FCS data.

The optimal CC position was determined for Alexa 405 in water and in each glycerol:water mixture by varying the position until the highest photon count rate (k) was achieved, which corresponded to the curves with greatest $G(0)$ amplitude. This has to be done at a fixed focal depth, and here we used 100 μm (where this was the distance from the bottom of the cover glass to the centre of the focal spot in the sample). The data collected for each mixture as a function of CC position compared against Alexa in water are shown in Figure 3. The plot shows, as expected, very large changes in signal amplitude as the CC position was changed and that the degree of correction increased as the viscosity/RI increased. Ultimately, what is important here is that if one is analysing a heterogenous system with varying viscosity at a fixed focal depth, then the $G(0)$ amplitude will be unreliable. This means that extracting accurate concentration information when scanning (or imaging) across a heterogenous sample one needs to adjust the CC position as the RI varies. However, the extent to which the corrections can be implemented is limited by RI change, as here corrections could only be applied up to 40% glycerol.

¹ We do not have the capability to measure RI at 422 nm.



1
2 **Figure 3. (a)** Non-optimized CC position: ACFs obtained for Alexa 405 in the glycerol:water mixtures
3 from (from 10 to 50% glycerol) with focal depth = 100 μm and CC = 0.13; **(b)** Plot of $G(0)$ magnitude
4 as a function of CC position for each glycerol:water mixture at 100 μm focal depth. The red dotted line
5 represents the average amplitude obtained for Alexa 405 in water at the optimized CC position (0.13).
6 **(c)** Optimized CC position: ACFs obtained for Alexa 405 in the various solutions at the optimized (RI-
7 corrected) CC position for each sample; **(d)** Comparison between the parameters recovered for Alexa
8 405 when samples were measured at 100 μm focal depth and optimized CC position for each mixture
9 as in Table 2 (filled circles) and at 10 μm and fixed CC=0.13 (open diamonds). The apparent D_{coeff} thus
10 recovered is shown in blue solid lines and the apparent concentration, in dashed red. Concentration of
11 Alexa 405 in all solutions was 10 nM and data was collected at 20 $^{\circ}\text{C}$, $n = 9$.

12
13 The effect of not correcting for RI with increasing viscosity are shown in Figure 3a
14 where all the data (with solutions of the same Alexa concentration) was collected at a fixed
15 correction collar setting (0.13 which was that determined for water) and at a fixed focal depth
16 of 100 μm . This means that any concentration information extracted will be very unreliable.
17 Figure 3b shows data collected at every CC position for each glycerol:water mixture. The
18 corrected data, Figure 3c, shows the dramatic improvement in the raw data which will generate
19 accurate concentration values when the correct CC position is used.

20 In Figure 3d we compare the quantitative values extracted from the ACF data obtained
21 using the individually optimized CC settings, with data collected at a fixed CC = 0.13 and a

focal depth of 10 μm . The plot shows that the recovered D_{coeff} is nearly identical independent of focal depth and CC, but that the fluorophore concentrations recovered in both cases vary greatly. The apparent increase in concentration for the corrected data is due to the fluorescent impurity in the glycerol, which can be accounted for. The much higher concentrations from the unoptimized measurements is probably due to increased light scatter being collected.

The FCS data collected under optimized conditions, i.e., combination of appropriate focal depth and CC position, was used to quantify the viscosity-diffusion dependence for Alexa 405 (Table 2). The D_{coeff} of Alexa 405 decreased from $333 \mu\text{m}^2\text{s}^{-1}$ (water) to $44 \mu\text{m}^2\text{s}^{-1}$ (5:5 glycerol:water), whilst the apparent concentration increased, from 11.5 to 14.8 nM which was due to the contribution of the glycerol impurity. When measured with carefully controlled CC settings the recovered D_{coeff} values were in good agreement with the theoretical values (Table 2). Using the mean D_{coeff} of Alexa 405 in water, $333 \pm 16 \mu\text{m}^2\text{s}^{-1}$, we determined its R_H to be 6.4 \AA . However, FCS measurements and data fitting to single species model showed an increase in fluorophore concentration, which we attributed to the presence of the fluorescent impurity in glycerol. A two species 3D Gaussian diffusion model which could potentially separate species that differ in size, assuming that they have the same molecular brightness [53] was attempted but this too failed to fit the data. Thus, we deduced that this fluorescent impurity and Alexa 405 were similar in size but had different molecular brightness.

Table 2. Diffusion coefficient (D_{coeff}) and concentration (C) parameters recovered from the ACFs for 10 nM Alexa 405 in water and in different glycerol:water mixtures, all at a 100 μm focal depth. All curves were fitted to a 1 species 3D Gaussian diffusion model. $n = 9$. Corrected concentration accounts for glycerol impurity.

Gly:water ratio	η_{exp} (cP) ^a	η_{theory} (cP) ^b	Exp. $D_{\text{coeff}} \pm \text{SD}$ ($\mu\text{m}^2\text{s}^{-1}$)	Theor. D_{coeff} ($\mu\text{m}^2\text{s}^{-1}$) ^c	$C \pm \text{St Dev}$ (nM)	Corrected C (nM)	CC setting
0:1	1.00	1.00	333±16	-	11.5±1	11.5	0.13
1:9	1.38	1.37	242±8	242	10.9±0.2	9.9	0.15
2:8	1.98	1.97	169±6	169	12.4±0.2	11	0.17
3:7	3.13	2.97	107±4	112	12.1±0.2	10.1	0.17
4:6	4.86	4.77	69±3	70	12.7±0.9	10.3	0.19
5:5	7.62	8.27	44±1	41	14.8±0.4	12	0.21

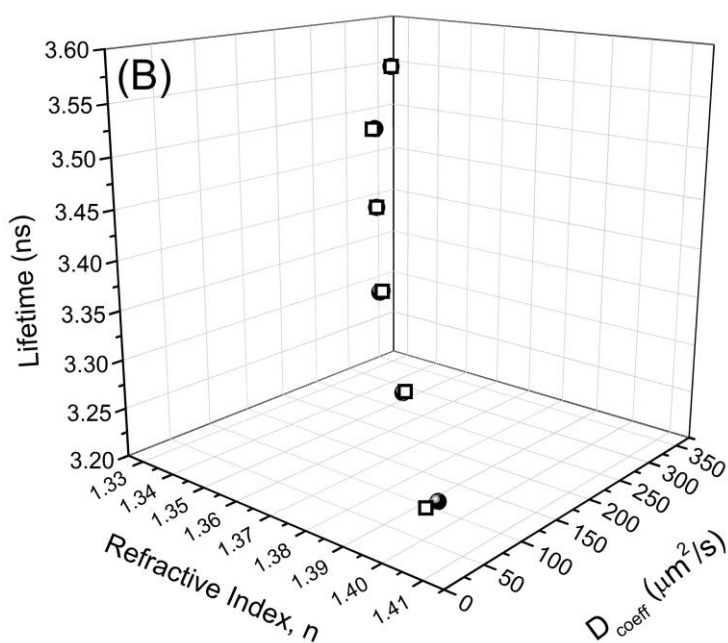
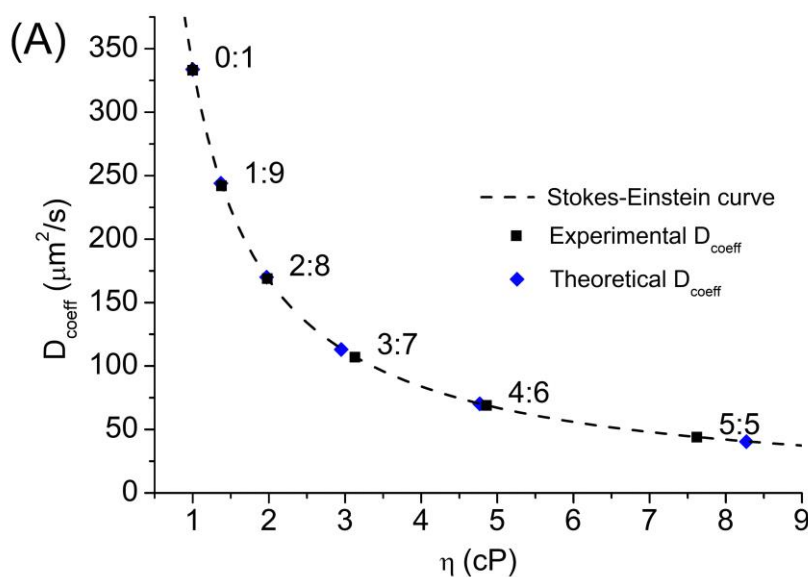
^aViscosity calculated using the Stokes-Einstein formula and the FCS-recovered Exp. D_{coeff} , assuming constant $R_H = 6.4 \text{\AA}$ for Alexa 405. ^bTheoretical viscosity η_{theory} of each glycerol:water mixture calculated according to reference [54]. ^cTheoretical D_{coeff} calculated using the Stokes-Einstein relationship and η_{theory} (assuming R_H (Alexa 405) = 6.4 \AA).

To prove this, we a photon counting histogram (PCH) analysis on the blank glycerol:water mixtures and were able to determine that the impurity had an estimated molecular brightness of $\sim 1290 \pm 82$ cps, which was $\sim 75\%$ as bright as Alexa in water (**Figure S6** and **Table S4** in **SI**). Furthermore, we estimated that the impurity was present at a concentration of ~ 5.6 nM in pure glycerol. When this information was combined with the FCS recovered concentration for Alexa, we were able to correct for the presence of the impurity. By adding the FCS-recovered concentration for a 10 nM Alexa 405 aqueous solution (11.5 nM,

1 Table 2) with the PCH-recovered impurity concentration for the glycerol:water 5:5 blank
2 solution (2.8 nM), we obtain 14.3 nM which was in good agreement with the recovered
3 concentration for the Alexa-containing 5:5 mixture (14.8 nM, as per Table 2).

4 If we assume that Alexa 405 has a constant R_H in the range of 1:9 to 5:5 glycerol:water
5 ratios, then the Stokes-Einstein relationship can be used to estimate the solution viscosity and
6 this is another way to validate our results as the solution viscosity is known. With the
7 experimental FCS-recovered D_{coeff} values we calculated the expected viscosity η_{exp} of each
8 mixture, whilst the theoretical viscosity η_{theory} , calculated according to reference [54] was used
9 to determine the theoretical D_{coeff} . We then plotted the theoretical and experimental data for
10 the dependence of the fluorophore diffusion coefficient with solution viscosity over the 0.5 to
11 9 cP range (Figure 4a). There was good agreement between theory and experimental values
12 apart from the 5:5 glycerol:water mixture where we observed a greater deviation from both
13 η_{theory} (~ 8%) and the theoretical D_{coeff} (~ 7%). The discrepancy could be due to either an error
14 in sample preparation, or a significant increase in solution temperature for these measurements
15 or related to the glycerol impurity. The temperature dependence of glycerol's viscosity has
16 been widely reported [55,56] and can be significant over a 5-10°C range. However, the
17 measured temperatures in the laboratory were fairly constant (20 ± 1 °C) and the 405 nm source
18 is both weakly adsorbed by the solvent and is working at very low power, such that we do not
19 have a valid mechanism for local heating of the solvent. As this is the only data point with a
20 significant variance, it is more likely due to a preparation error, as measuring out accurate small
21 quantities of the viscous glycerol was technically a bit challenging. In hindsight, an orthogonal
22 measurement of viscosity is required here, to validate the value and remove the uncertainty.

23 However, the effect of the fluorescent glycerol impurity at higher concentration in the
24 5:5 glycerol:water mixture is the more likely explanation. By taking this into account, the
25 experimental D_{coeff} value for Alexa 405 in the 5:5 glycerol:water mixture can be corrected for
26 by using a simple relationship. With the brightness ϵ and concentration C of both Alexa 405
27 and the impurity known from the PCH data, we calculated the ratio between the products of
28 $\epsilon \times C$, which was 4.7:1 (Alexa 405:impurity). Then, one can model the FCS measured D_{coeff} as
29 $(4.7 \times D_{\text{coeff,A405}}) + (1 \times D_{\text{coeff,imp}})$, and by substituting FCS $D_{\text{coeff,A405}}$ for $44 \mu\text{m}^2\text{s}^{-1}$, and $D_{\text{coeff,imp}}$
30 for $53 \mu\text{m}^2\text{s}^{-1}$ (determined by fitting a 1 species 3D diffusion model to the data collected for
31 the 5:5 blank sample) we obtain $D_{\text{coeff,A405}} = 42 \mu\text{m}^2\text{s}^{-1}$. This is in better agreement with the
32 theoretical, $41 \mu\text{m}^2\text{s}^{-1}$ value. When this value was used to calculate viscosity, we obtained a
33 more accurate value of ~ 8 cP. These calculations would suggest that the alternative
34 explanation for deviations between the experimental and theoretical values caused by a change
35 (a decrease) in the hydrodynamic radius of Alexa 405 as the solvation shell changes with higher
36 glycerol concentrations was not significant here.



1
2 **Figure 4. (a)** Variation of the diffusion coefficient with viscosity (at 20 °C) for Alexa 405 in
3 water/glycerol mixtures. Experimental D_{coeff} values ($n = 9$) were determined by FCS (black filled
4 squares) and the theoretical D_{coeff} values (blue diamonds) were calculated by substituting the
5 theoretical viscosity η_{theory} in the SE relationship. In both cases we assumed a constant $R_h = 6.4 \text{ \AA}$.
6 The dashed line represents a Stokes-Einstein master curve calculated for a probe of $R_h = 6.4 \text{ \AA}$; (b)
7 3D plot of D_{coeff} as a function of RI and Lifetime, the theoretical (open squares) and experimental
8 (optimized CC position at 100 μm , black spheres) D_{coeff} overlap almost perfectly.
9

1 Figure 4b shows the 3D plot of D_{coeff} , (theoretical and the experimental), as a function
2 of RI and fluorescence lifetime. This demonstrates that Alexa 405 is well behaved (i.e.,
3 predicable) in water-glycerol mixtures and thus therefore should be suitable for studying other
4 systems over this range of viscosities and refractive indices. The very small deviation which
5 starts to arise as the glycerol concentration increases is indicative of a non-radiative pathway
6 becoming more significant as the polarity changes. This smooth 3D trajectory can be fitted
7 ($r^2=0.999$) to a simple polynomial ($z = 11.14 - 5.5261x - (3.964 \times 10^{-4})y$) where z =lifetime,
8 x =refractive index, and y = diffusion coefficient which should facilitate predicting behaviour
9 for intermediate viscosities. The predictability of the lifetime response in this region should
10 also facilitate accurate lifetime-based FRET measurements using Alexa 405 as a donor.
11
12

13 Conclusions

14 We have characterised in detail the photophysical behaviour of Alexa 405 in water and
15 water: glycerol mixtures to provide useful information for its use as an FCS probe with UV,
16 405 nm excitation. The relative fluorescence quantum yield (0.93 ± 0.02), lifetime (3.56 ± 0.010
17 ns), and diffusion coefficient ($D_0 = 333 \pm 16 \mu\text{m}^2\text{s}^{-1}$) in water of Alexa 405 are reported for the
18 first time. We assessed in detail its behaviour with respect to viscosity and refractive index
19 changes in a glycerol:water model system and its quantum yield remained essentially constant,
20 up to a 50% by volume glycol mixture. There was a linear dependence of fluorescence lifetime
21 with the inverse of the refractive index squared, but a significant, difference (18-20% lower)
22 from the lifetimes calculated using the Strickler-Berg model. This large deviation suggests that
23 there is a substantial solvent and potential hydrogen bonding effects which are to be expected
24 for these solvents and this fluorophore. Furthermore, lifetime data recorded from micromolar
25 concentration solutions showed the presence of a rise time in the decay curves which suggested
26 that Alexa 405 was aggregating as the glycerol concentration increased. Thus, the emission
27 photophysics warrants further, more detailed investigation. In particular the measurement of
28 absolute quantum yields and a study of the aggregation effects in less polar environments might
29 be necessary for a more complete understanding of its solution properties.

30 Despite the higher degree of light scatter with 405 nm excitation, accurate diffusion
31 coefficients, fluorophore concentrations, and thus solution viscosities can be reliably
32 determined up to ≈ 8 cP with $\sim 10\%$ error when corrections for refractive index mismatch (i.e.,
33 correction collar) and the presence of a fluorescent impurity in glycerol were implemented.
34 We have also shown that we can use normal spectroscopic grade glycerol for building viscosity
35 models and correct for the presence of the ubiquitous fluorescent impurity. It was determined
36 that the impurity concentration was ~ 5.6 nM, and that it had a molecular brightness with 405
37 nm excitation of ~ 1300 cps (for emission >420 nm). It must be noted that impurity
38 concentration will probably be both supplier and batch dependant, and that the molecular
39 brightness values reported here are instrument dependant. Purification of spectroscopic grade
40 glycerol to remove these impurities which avoids the use of complex vacuum distillations is
41 not widely described in the literature. Treatment with activated charcoal and alumina followed

Citation: Effects of viscosity and refractive index on the emission and diffusion properties of Alexa Fluor 405 using fluorescence correlation and lifetime spectroscopies., C. van Zanten, D. Melnikau, and A.G. Ryder. *Journal of Fluorescence*, 31(3), 835-845, (2021).
DOI: [10.1007/s10895-021-02719-y](https://doi.org/10.1007/s10895-021-02719-y)

1 by filtration might be suitable [57], however, this has not been validated from a spectroscopic
2 viewpoint. A potentially useful alternative for viscosity measurements has been suggested by
3 one of the manuscript reviewers. Their suggestion was to use column purified PEG solutions
4 of the appropriate molecular weight and concentration to produce the required viscosity as this
5 should be free from fluorescent impurities, although one needs then to consider fluorophore-
6 polymer interactions.

7 Thus, for FCS measurements in samples with homogenous viscosity, accurate diffusion
8 and concentration data can be extracted using 400 nm excitation. However, our studies show
9 clearly, that if imaging/scanning a sample with heterogenous viscosity where the refractive
10 index varies there is potential for error. Unless the correction collar is correctly set for each
11 focal point then the concentration data from FCS experiments will be unreliable, whereas the
12 diffusion coefficient is largely unaffected.

13 In conclusion, Alexa 405 has been shown to be a suitable fluorophore for FCS
14 measurements using 405 nm excitation. The fluorophore is also a reliable fluorescent standard
15 for the measurement of the confocal volume when using 405 nm laser diode excitation sources.
16 Its stable spectral behaviour also indicates that it would be very suitable for multi-parameter
17 use as a dual colour FRET probe [33].

18
19

Citation: Effects of viscosity and refractive index on the emission and diffusion properties of Alexa Fluor 405 using fluorescence correlation and lifetime spectroscopies., C. van Zanten, D. Melnikau, and A.G. Ryder. *Journal of Fluorescence*, 31(3), 835-845, (2021).
DOI: [10.1007/s10895-021-02719-y](https://doi.org/10.1007/s10895-021-02719-y)

1

2 **Acknowledgements**

3 This publication has emanated from research supported in part by a research grant from CAPES
4 (Grant No. BEX 1415-15-8) and from Science Foundation Ireland (SFI) which was co-funded
5 under the European Regional Development Fund under Grant number (14/IA/2282, Advanced
6 Analytics for Biological Therapeutic Manufacture, to AGR). The FCS instrumentation was
7 provided under an Irish Health Research Board Equipment Grant (EQ/2004/29).

8

9 **Supplementary Information (SI)**

10 Supplementary information is available [HERE](#) from the publisher.

11

12 **References**

- 13 1. Balbo J, Mereghetti P, Herten DP, Wade RC (2013) The shape of protein crowders is a major
14 determinant of protein diffusion. *Biophys J* 104 (7):1576-1584. doi:10.1016/j.bpj.2013.02.041
- 15 2. Pack CG, Nishimura G, Tamura M, Aoki K, Taguchi H, Yoshida M, Kinjo M (1999)
16 Analysis of Interaction Between Chaperonin GroEL and its Substrate Using Fluorescence
17 Correlation Spectroscopy. *Cytometry* 36
18 (3):247-253
- 19 3. Nolan R, Iliopoulou M, Alvarez L, Padilla-Parra S (2018) Detecting protein aggregation and
20 interaction in live cells: A guide to number and brightness. *Methods* 140-141:172-177.
21 doi:10.1016/j.ymeth.2017.12.001
- 22 4. Rezgui R, Blumer K, Yeoh-Tan G, Trexler AJ, Magzoub M (2016) Precise quantification of
23 cellular uptake of cell-penetrating peptides using fluorescence-activated cell sorting and
24 fluorescence correlation spectroscopy. *Biochim Biophys Acta* 1858 (7 Pt A):1499-1506.
25 doi:10.1016/j.bbamem.2016.03.023
- 26 5. Mittag JJ, Milani S, Walsh DM, Radler JO, McManus JJ (2014) Simultaneous measurement
27 of a range of particle sizes during Aβ₁₋₄₂ fibrillogenesis quantified using fluorescence
28 correlation spectroscopy. *Biochem Biophys Res Commun* 448 (2):195-199.
29 doi:10.1016/j.bbrc.2014.04.088
- 30 6. Wang F, Shi Y, Luo S, Chen Y, Zhao J (2012) Conformational Transition of Poly(N-
31 isopropylacrylamide) Single Chains in Its Cononsolvency Process: A Study by Fluorescence
32 Correlation Spectroscopy and Scaling Analysis. *Macromolecules* 45 (22):9196-9204.
33 doi:10.1021/ma301780f
- 34 7. Dominguez-Medina S, Chen S, Blankenburg J, Swanglap P, Landes CF, Link S (2016)
35 Measuring the Hydrodynamic Size of Nanoparticles Using Fluctuation Correlation
36 Spectroscopy. *Annu Rev Phys Chem* 67:489-514. doi:10.1146/annurev-physchem-040214-
37 121510

Citation: Effects of viscosity and refractive index on the emission and diffusion properties of Alexa Fluor 405 using fluorescence correlation and lifetime spectroscopies., C. van Zanten, D. Melnikau, and A.G. Ryder. *Journal of Fluorescence*, 31(3), 835-845, (2021).
DOI: [10.1007/s10895-021-02719-y](https://doi.org/10.1007/s10895-021-02719-y)

- 1 8. Cedervall T, Lynch I, Foy M, Berggard T, Donnelly SC, Cagney G, Linse S, Dawson KA
2 (2007) Detailed identification of plasma proteins adsorbed on copolymer nanoparticles.
3 *Angewandte Chemie* 46 (30):5754-5756. doi:10.1002/anie.200700465
- 4 9. Watanabe C, Yanagisawa M (2018) Cell-size confinement effect on protein diffusion in
5 crowded poly(ethylene)glycol solution. *Phys Chem Chem Phys* 20 (13):8842-8847.
6 doi:10.1039/c7cp08199e
- 7 10. Haidekker MA, Ling, T., Anglo, M., Stevens, H. Y., Frangos, J. A., Theodorakis, E. A.
8 (2001) New Fluorescent Probes for the Measurement of Cell Membrane Viscosity. *Chemistry*
9 *& Biology* 8:123-131
- 10 11. Weissberg SG, Simha, R., Rothman, S. (1951) Viscosity of Dilute and Moderately
11 Concentrated Polymer Solutions. *Journal of Research of the National Bureau of Standards*
12 47:298-314
- 13 12. Wöll D (2014) Fluorescence Correlation Spectroscopy in Polymer Science. *RSC Advances*
14 4 (5):2447-2465
- 15 13. Ota C, Noguchi S, Nagatoishi S, Tsumoto K (2016) Assessment of the Protein-Protein
16 Interactions in a Highly Concentrated Antibody Solution by Using Raman Spectroscopy.
17 *Pharm Res* 33 (4):956-969. doi:10.1007/s11095-015-1842-8
- 18 14. Ota C, Noguchi S, Tsumoto K (2015) The Molecular Interaction of a Protein in Highly
19 Concentrated Solution Investigated by Raman Spectroscopy. *Biopolymers* 103 (4):237-246.
20 doi:10.1002/bip.22593
- 21 15. Garidel P, Pevestorf B, Bahrenburg S (2015) Stability of buffer-free freeze-dried
22 formulations: A feasibility study of a monoclonal antibody at high protein concentrations.
23 *European Journal of Pharmaceutics and Biopharmaceutics* 97:125-139.
24 doi:10.1016/j.ejpb.2015.09.017
- 25 16. Szasz C, Alexa A, Toth K, Rakacs M, Langowski J, Tompa P (2011) Protein Disorder
26 Prevails under Crowded Conditions. *Biochemistry* 50 (26):5834-5844. doi:10.1021/bi200365J
- 27 17. Enderlein J, Gregor I, Patra D, Dertinger T, Kaupp UB (2005) Performance of fluorescence
28 correlation spectroscopy for measuring diffusion and concentration. *Chemphyschem* 6
29 (11):2324-2336. doi:10.1002/cphc.200500414
- 30 18. Chattopadhyay K, Saffarian S, Elson EL, Frieden C (2005) Measuring unfolding of proteins
31 in the presence of denaturant using fluorescence correlation spectroscopy. *Biophys J* 88
32 (2):1413-1422. doi:10.1529/biophysj.104.053199
- 33 19. Lehmann S, Seiffert S, Richter W (2015) Refractive Index Mismatch Can Misindicate
34 Anomalous Diffusion in Single-Focus Fluorescence Correlation Spectroscopy. *Macromol*
35 *Chem Phys* 216 (2):156-163. doi:10.1002/macp.201400349
- 36 20. Banachowicz E, Patkowski A, Meier G, Klamecka K, Gapinski J (2014) Successful FCS
37 experiment in nonstandard conditions. *Langmuir* 30 (29):8945-8955. doi:10.1021/la5015708
- 38 21. Wang S, Arena, E. T., Eliceiri, K. W., Yuan, M. (2018) Automated and Robust
39 Quantification of Colocalization in Dual-Color Fluorescence Microscopy: A Nonparametric
40 Statistical Approach. *IEEE Transactions on Image Processing* 27 (2):622-636

Citation: Effects of viscosity and refractive index on the emission and diffusion properties of Alexa Fluor 405 using fluorescence correlation and lifetime spectroscopies., C. van Zanten, D. Melnikau, and A.G. Ryder. *Journal of Fluorescence*, 31(3), 835-845, (2021).
DOI: [10.1007/s10895-021-02719-y](https://doi.org/10.1007/s10895-021-02719-y)

- 1 22. Chung HS, Meng, F., Kim, JY., McHale, K., Gopich, I. V., Louis, J. M. (2017)
- 2 Oligomerization of the tetramerization domain of p53 probed by two- and three-color single-
- 3 molecule FRET. *PNAS* 114 (33):E6812-E6821
- 4 23. Chung HS, McHale, K., Louis, J. M., Eaton, W. A. (2012) Single-Molecule Fluorescence
- 5 Experiments Determine Protein Folding Transition Path Times. *Science* 335:981-984
- 6 24. Szczurek AT, Prakash, K., Lee, H-K., Żurek-Biesiada, D. J., Best, G., Hagmann, M.,
- 7 Dobrucki, J. W., Cremer, C., Birk, U. (2014) Single molecule localization microscopy of the
- 8 distribution of chromatin using Hoechst and DAPI fluorescent probes. *Nucleus* 5 (4):331-334-
- 9 25. Girkin JM, Ferguson, A. I., Wokosin D. L., Gurney A. M. (2000) Confocal microscopy
- 10 using an InGaN violet laser diode at 406 nm. *Optics Express* 7 (10)
- 11 26. Luo D, Kuang C, Liu X, Wang G (2013) Experimental investigations on fluorescence
- 12 excitation and depletion of ATTO 390 dye. *Optics & Laser Technology* 45:723-725.
- 13 doi:10.1016/j.optlastec.2012.05.003
- 14 27. S. Ruttinger VB, B. Kramer, R. Erdmann, R. Macdonald, F. Koberling (2008) Comparison
- 15 and accuracy of methods to determine the confocal volume for quantitative fluorescence
- 16 correlation spectroscopy. *Journal of Microscopy* 232 (2):343–352
- 17 28. Resch-Genger U, Rurack K (2013) Determination of the photoluminescence quantum yield
- 18 of dilute dye solutions (IUPAC Technical Report). *Pure and Applied Chemistry* 85 (10):2005-
- 19 2013. doi:10.1351/pac-rep-12-03-03
- 20 29. Muller P, Schwille P, Weidemann T (2014) PyCorrFit-generic data evaluation for
- 21 fluorescence correlation spectroscopy. *Bioinformatics* 30 (17):2532-2533.
- 22 doi:10.1093/bioinformatics/btu328
- 23 30. Strickler SJ, Berg RA (1962) Relationship between Absorption Intensity and Fluorescence
- 24 Lifetime of Molecules. *The Journal of Chemical Physics* 37 (4):814-822.
- 25 doi:10.1063/1.1733166
- 26 31. Topygin D, Savtchenko RS, Meadow ND, Roseman S, Brand L (2002) Effect of the
- 27 Solvent Refractive Index on the Excited-State Lifetime of a Single Tryptophan Residue in a
- 28 Protein. *Journal of Physical Chemistry B* 106 (14):3724-3734
- 29 32. Fisher TR, Zhou G, Shi Y, Huang L (2020) How does hydrogen bond network analysis
- 30 reveal the golden ratio of water–glycerol mixtures? *PCCP* 22 (5):2887-2907.
- 31 doi:10.1039/C9CP06246G
- 32 33. Song D, Yang R, Fang SY, Liu YP, Long F (2018) A FRET-based dual-color evanescent
- 33 wave optical fiberaptasensor for simultaneous fluorometric determination of aflatoxin M1 and
- 34 ochratoxin A. *Microchimica Acta* 185 (11):10. doi:10.1007/s00604-018-3046-5
- 35 34. Tanahashi T, Kawaguchi M, Honda T, Takahashi A (1994) Adsorption of poly(N-
- 36 isopropylacrylamide) on silica surfaces. *Macromolecules* 27 (2):606-607.
- 37 doi:10.1021/ma00080a040
- 38 35. Callewaert M, Grandfils C, Boulangé-Petermann L, Rouxhet PG (2004) Adsorption of
- 39 poly(N-isopropylacrylamide) on glass substrata. *J Colloid Interface Sci* 276 (2):299-305.
- 40 doi:10.1016/j.jcis.2004.03.063

Citation: Effects of viscosity and refractive index on the emission and diffusion properties of Alexa Fluor 405 using fluorescence correlation and lifetime spectroscopies., C. van Zanten, D. Melnikau, and A.G. Ryder. *Journal of Fluorescence*, 31(3), 835-845, (2021).
DOI: [10.1007/s10895-021-02719-y](https://doi.org/10.1007/s10895-021-02719-y)

- 1 36. Gao J, Hu TJ, Zhang YB, Li P, Wu C (1999) The adsorption of linear poly(N-
2 isopropylacrylamide) chains on surfactant-free polystyrene nanoparticles. *Chin J Polym Sci* 17
3 (6):595-601
- 4 37. Meaney PM, Fox CJ, Geimer SD, Paulsen KD (2017) Electrical Characterization of
5 Glycerin: Water Mixtures: Implications for Use as a Coupling Medium in Microwave
6 Tomography. *IEEE Transactions on Microwave Theory and Techniques* 65 (5):1471-1478
- 7 38. Jr. GEM, Quinn RG, Litovitz TA (1962) Dielectric Properties of Glycerol—Water
8 Mixtures. *The Journal of Chemical Physics* 37 (2):239-242. doi:10.1063/1.1701311
- 9 39. Racknor C, Singh MR, Zhang YN, Birch DJS, Chen Y (2014) Energy transfer between a
10 biological labelling dye and gold nanorods. *Methods and Applications in Fluorescence* 2 (1):6.
11 doi:10.1088/2050-6120/2/1/015002
- 12 40. Krishna MMG (1999) Excited-State Kinetics of the Hydrophobic Probe Nile Red in
13 Membranes and Micelles. *The Journal of Physical Chemistry A* 103 (19):3589-3595
- 14 41. Behrends R, Fuchs, K., Kaatze, U., Hayashi, Y., Feldman, Y. (2006) Dielectric properties
15 of glycerol/water mixtures at temperatures between 10 and 50 °C. *The Journal of Chemical*
16 *Physics* 124
- 17 42. Rurack K, Spieles M (2011) Fluorescence quantum yields of a series of red and near-
18 infrared dyes emitting at 600-1000 nm. *Anal Chem* 83 (4):1232-1242. doi:10.1021/ac101329h
- 19 43. Casamayou-Boucau Y, Ryder AG (2018) Accurate anisotropy recovery from fluorophore
20 mixtures using Multivariate Curve Resolution (MCR). *Anal Chim Acta* 1000:132-143.
21 doi:10.1016/j.aca.2017.11.031
- 22 44. Freire S, de Araujo MH, Al-Soufi W, Novo M (2014) Photophysical study of Thioflavin T
23 as fluorescence marker of amyloid fibrils. *Dyes and Pigments* 110:97-105.
24 doi:10.1016/j.dyepig.2014.05.004
- 25 45. Gafni A, Brand, L. (1976) Fluorescence Decay Studies of Reduced Nicotinamide Adenine
26 Dinucleotide in Solution and Bound to Liver Alcohol Dehydrogenase. *Biochemistry* 15
27 (15):3165-3171
- 28 46. Gaiduk A, Ruijgrok, P. V., Yorulmaz, M., Orrit, M. (2011) Making gold nanoparticles
29 fluorescent for simultaneous absorption and fluorescence detection on the single particle level.
30 *Physical Chemistry Chemical Physics* 13:149–153
- 31 47. Chattopadhyay PK, Gaylord, B., Palmer, A., Jiang, N., Raven, M. A., Geoff, L. , Reuter,
32 M. A., A.K.M. Rahman, N., Price, D. A., Betts, M. R. , Roederer, M. (2012) Brilliant Violet
33 Fluorophores: A New Class of Ultrabright Fluorescent Compounds for Immunofluorescence
34 Experiments. *Cytometry Part A* 81A:456-466
- 35 48. Telford W, Kapoor V, Jackson J, Burgess W, Buller G, Hawley T, Hawley R (2006) Violet
36 laser diodes in flow cytometry: an update. *Cytometry A* 69 (11):1153-1160.
37 doi:10.1002/cyto.a.20340
- 38 49. Stefl M, Benda A, Gregor I, Hof M (2014) The fast polarization modulation based dual-
39 focus fluorescence correlation spectroscopy. *Opt Express* 22 (1):885-899.
40 doi:10.1364/OE.22.000885
- 41 50. P. Muller PS, T. Weidemann (2014) PyCorrFit—generic data evaluation for fluorescence
42 correlation spectroscopy. *Bioinformatics Applications Note* 30 (17):2532–2533

Citation: Effects of viscosity and refractive index on the emission and diffusion properties of Alexa Fluor 405 using fluorescence correlation and lifetime spectroscopies., C. van Zanten, D. Melnikau, and A.G. Ryder. *Journal of Fluorescence*, 31(3), 835-845, (2021).
DOI: [10.1007/s10895-021-02719-y](https://doi.org/10.1007/s10895-021-02719-y)

- 1 51. Müller CB, Loman A, Pacheco V, Koberling F, Willbold D, Richtering W, Enderlein J
- 2 (2008) Precise measurement of diffusion by multi-color dual-focus fluorescence correlation
- 3 spectroscopy. *EPL (Europhysics Letters)* 83 (4):46001. doi:10.1209/0295-5075/83/46001
- 4 52. Diaspro A, Federici, F., Robello, M. (2002) Influence of Refractive Index Mismatch in
- 5 high-resolution three-dimensional confocal microscopy. *Applied Optics* 41 (4):685-690
- 6 53. Meseth U, Wohland, T., Rigler, R., Vogel, H. (1999) Resolution of Fluorescence
- 7 Correlation Measurements. *Biophysical Journal* 76:1619-1631
- 8 54. Volk A, Kahler CJ (2018) Density model for aqueous glycerol solutions Andreas. *Exp*
- 9 *Fluids* 59 (5):4. doi:10.1007/s00348-018-2527-y
- 10 55. Cook RL, Jr. HEK, Herbst CA, Herschbach DR (1994) Pressure and temperature dependent
- 11 viscosity of two glass forming liquids: Glycerol and dibutyl phthalate. *The Journal of Chemical*
- 12 *Physics* 100 (7):5178-5189. doi:10.1063/1.467276
- 13 56. Ferreira AGM, Egas APV, Fonseca IMA, Costa AC, Abreu DC, Lobo LQ (2017) The
- 14 viscosity of glycerol. *The Journal of Chemical Thermodynamics* 113:162-182.
- 15 doi:<https://doi.org/10.1016/j.jct.2017.05.042>
- 16 57. Armarego WLF, Chai CLL (2003) *Purification of Laboratory Chemicals*. 5th edn.
- 17 Butterworth-Heinemann,
- 18